Institute of Special Wild Economic Animals and Plants[1], Chinese Academy of Agriculatural Sciences; College of Chinese Medicinal Materials[2], Jilin Agricultural University; Norman Bethune College of Medicine[3], Jilin University, Changchun City, China

Bioconversion of ginsenoside Rd to ginsenoside M1 by snailase hydrolysis and its enhancement effect on insulin secretion *in vitro*

Wei Li[1,2,3], Zi Wang[2], Jian Gu[3], Li Chen[3], Wei Hou[1], Yinping Jin[1], Yingping Wang[1]

Received September 19, 2014, accepted October 17, 2014

Professor Ying-ping Wang, Institute of Special Wild Economic Animals and Plant, Chinese Academy of Agriculatural Sciences, Changchun 132109 China
yingpingw@126.com

Pharmazie 70: 340–346 (2015) *doi: 10.1691/ph.2015.4797*

In the present work, we report efficient production of ginsenoside M1 (G-M1) from ginsenoside Rd (G-Rd) by snailase hydrolysis using response surface methodology (RSM). During investigation of the hydrolysis of ginsenoside Rd by various glycoside hydrolases, snailase showed a strong ability to transform G-Rd into G-M1 with 100% conversion. RSM was used to optimize the effects of the reaction temperature, enzyme load, and reaction time on the conversion process. Validation of the RSM model was verified by the good agreement between the experimental and the predicted values of G-M1 conversion yield. The optimum preparation conditions were as follows: temperature of 41.0°C; enzyme load of 17.5 %; reaction time of 18 h. The determined method may be highly applicable for the enzymatic preparation of G-M1 for medicinal purpose. Furthermore, the effect of G-M1 on insulin secretion in MIN6 pancreatic β-cells was investigated.

1. Introduction

Ginseng (the roots of *Panax ginseng* C. A. Meyer) has been considered as one of the most famous traditional medicines in Asian countries (Qi et al. 2011). The pharmacological properties of ginseng are mainly attributed to ginsenosides, which are classified into protopanaxadiol-type ginsenosides and protopanaxatriol-type ginsenosides based on sapogenins (Wan et al. 2008). It is well known that protopanaxadiol-type ginsenosides such as ginsenoside Rd (G-Rd), Rb1 and Rc are metabolized by intestinal bacteria after oral administration into their final derivative, 20-*O*-β-D-glucopyranosyl-20(*S*)-protopanaxadiol (also called ginsenoside M1 or Compound K) (Wakabayashi et al. 1997; Akao et al. 1998). Ginsenoside M1 (G-M1) is the genuine active form of protopanaxadiol-type ginsenosides, and it has received increasing attention in view of various biological activities against-cancer (Lee et al. 2010; Kim, et al. 2009), inflammation (Joh et al. 2011), and diabetes (Yoon et al. 2007; Kim et al. 2009).

Several reports have shown that efficient production of minor ginsenosides including Rh1, Rg2, and F1 is reliable and feasible (Ko et al. 2003). Among preparation methods such as enzymatic conversion (Liu et al. 2010), mild acid hydrolysis (Han et al. 1982) and microbial conversion (Bae et al. 2002; Wang et al. 2011), enzymatic preparation (EP) has been implicated as the most efficient transformation technique for minor ginsenoside production. EP was used for the preparation of active constituents *via* the selective hydrolysis of the sugar moieties, owing to its high specificity, yield and productivity. Recently, snailase (a complex of cellulase, hemicellulase, pectinase and β-glucuronidase), extracted from the digestive tract of snails (You et al. 2011), have received increasing attention due to strong hydrolysis ability (Liu et al. 2005). In our previous paper, we have employed snailase to transform crude protopanaxadiol-type ginsenosides to G-M1 with great success (Li et al. 2011). In the present study, we report efficient preparation of G-M1 using snailase hydrolysis from G-Rd, a main ginsenoside of protopanaxadiol-type ginsenosides. Response surface methodology (RSM), an effective statistical technique, can be used to evaluate multiple parameters and their interactions by establishing a mathematical model (Liu et al. 2013). Prior to this study, we have widely employed RSM to optimize the extraction of natural components from herbal medicines (Li et al. 2011; Zhao et al. 2012).

In this work, we investigated the feasibility of using snailase hydrolysis to preparing G-M1 *via* biotransformation of G-Rd. The effects of reaction temperature, enzyme load, and reaction time on the snailase hydrolysis efficiency and their interactions were also systemically analyzed for the first time with RSM method. Furthermore, the effect of G-M1 on insulin secretion in MIN6 pancreatic β-cells was investigated.

2. Investigations and results

2.1. Selection of glycolytic enzymes

To select enzymes for the concurrent bioconversion of G-Rd into G-M1, the hydrolyzing ability of several glycolytic enzymes including snailase, β-glucanase, cellulase and amylase, were evaluated. Individual kinetics of hydrolysis of 20 mg/mL G-Rd were investigated incubating each glycolytic enzyme at 37 °C for 24 h. In addition to cellulase and amylase, snailase and β-glucanase gave the same hydrolysis ability. However, complete hydrolysis of Rd was only achieved in 24 h by snailase (data not shown). Therefore, snailase was selected to carry out the next investigation.

Table 1: Box-Behnken experimental design with the independent variables

Run	Coded variables levels			*Y G-M1 (mg/mL)*	
	X_1, Reaction temperature (°C)	X_2, Enzyme load (%)	X_3, Reaction time (h)	Actual	Predicted
1	−1 (35)	−1 (5.0)	0 (14)	2.55	3.47
2	1 (50)	−1 (5.0)	0 (14)	2.45	2.36
3	−1 (35)	1 (20)	0 (14)	9.89	9.99
4	1 (50)	1 (20)	0 (14)	8.86	7.95
5	−1 (35)	0 (12.5)	−1 (4)	2.55	1.94
6	1 (50)	0 (12.5)	−1 (4)	2.78	3.18
7	−1 (35)	0 (12.5)	1 (24)	9.66	9.26
8	1 (50)	0 (12.5)	1 (24)	4.26	4.87
9	0 (42.5)	−1 (5.0)	−1 (4)	2.17	1.86
10	0 (42.5)	1 (20)	−1 (4)	5.37	5.88
11	0 (42.5)	−1 (5.0)	1 (24)	4.84	4.33
12	0 (42.5)	1 (20)	1 (24)	12.11	12.42
13	0 (42.5)	0 (12.5)	0 (14)	12.54	12.50
14	0 (42.5)	0 (12.5)	0 (14)	12.48	12.50
17	0 (42.5)	0 (12.5)	0 (14)	12.39	12.50

2.2. Model fitting

After the preliminary ranges of the preparation variables were determined by one-factor-at-a-time experiment, the three independent variables, the reaction temperature (X_1, 35-50 °C), enzyme load (X_2, 5-20 %) and reaction time (X_3, 4-24 h), were fixed to optimize the yields of G-M1. The whole design consisted of 15 experimental points as listed in Table 1, and three replicates (run 13-15) at the center of the design were used for estimating the experimental error sum of squares. The triplicates were performed at all design points in randomized order.

As Table 2 showed, the analysis of variance (ANOVA) of conversion yield of G-M1 indicated that experimental data had a determination coefficient (R^2) of 0.9881 with the calculated model with no significant lack of fit (P = 0.00038). That means that the calculated model was able to explain 98.81 % of the results. The results indicated that the model used to fit response variables was significant ($P < 0.0001$) and adequate to represent the relationship between the response and the independent variables. *F*-test suggested that the model had a very high model *F*-value ($F = 64.65$), indicating high significance. R^2_{adj} value (adjusted determination coefficient) is the correlation measure for testing the goodness-of-fit of the regression equation (Li et al. 2011; Zhao et al. 2012). The R^2_{adj} value of this model is 0.9728, which indicated only 2.72 % of the total variations were not explained by model. Meanwhile, a relatively lower value of coefficient of variation (CV = 4.35) showed a better precision and reliability of the experiments carried out (Zhao et al. 2012) SS, sum of squares; DF, degree of freedom; MS, mean square

It can be seen in Table 3 that conversion yield of G-M1 was affected most significantly by enzyme load (X_2) and reaction time (X_3) ($P < 0.0001$), followed by reaction temperature (X_1) ($P = 0.0175$). It was evident that all the quadratic parameters (*X2 1*, *X2 2*, *X2 3*) were significant at the level of $P < 0.0001$, whereas all the interaction quadratic parameters were insignificant ($P > 0.0001$). Predicted response *Y* for the yield of G-M1 could be expressed by the following second-order polynomial equation in term of coded values.

$$Y = -143.3 + 6.16X_1 + 1.56X_2 + 1.90X_3 - 4.133E{-}003X_1X_2 - 0.019X_1X_3 + 0.0136X_2X_3 - 0.7X_1^2 - 0.047X_2^2 - 0.04X_3^2$$

Where *Y* is the yield of G-M1 (mg/mL), and X_1, X_2 and X_3 are the coded variables for reaction temperature, enzyme load and reaction time, respectively.

2.3. Analysis of response surface

The regression equation was graphically represented by 3D response surface and 2D contour plots. From three dimensional response surface curves and contour plots shown in Figs. 1–3, the effects of the independent variables and their mutual interaction on the yield of G-M1 can be seen.

Figure 1 shows the interaction between reaction temperature (X_1) and enzyme load (X_2) on the yield of G-M1. Increase in reaction temperature from 35 to 50 °C with enzyme load from 5 to 20 % enhanced the conversion yield of G-M1. While with increase of reaction temperature over 40 °C there was a gradual decline in the response and enzyme load over 20 % did not show any obvious effect on the yield of G-M1. It could be explained that, increasing reaction temperature may enhance snailase activity in preparation process (Liu et al. 2010).

Figure 2 depictes the effect of reaction temperature (X_1) and reaction time (X_3) on the yield of G-M1. As shown Fig. 2, it may be also observed that increase of reaction temperature from 35 to 50 °C and reaction time from 4 to 19 h, gradually increased the yield of G-M1. However, there was also a decrease in G-M1 yield over a reaction temperature of 40 °C and reaction time more than 19 h.

Table 2: Analysis of variance for the fitted quadratic polynomial model

Source	SS	DF	MS	*F*-value	Prob > F	
Model	302.05	9.00	33.56	64.65	< 0.0001	significant
Residual	3.63	7.00	0.52			
Lack of fit	3.47	3.00	1.16	28.05	0.0038	insignificant
Pure error	0.16	4.00	0.04			

Table 3: Estimated regression model of relationship between response variables (Y) and independent variables (X_1, X_2, X_3)

Variables	DF	SS	MS	F-values	p-value
X_1	1	4.96	4.96	9.56	0.0175
X_2	1	73.33	73.33	141.25	<0.0001
X_3	1	40.50	40.50	78.01	<0.0001
X_1X_2	1	0.22	0.22	0.42	0.5393
X_1X_3	1	7.92	7.92	15.26	0.0058
X_2X_3	1	4.14	4.14	7.98	0.0256
X^2_1	1	65.27	65.27	125.73	<0.0001
X^2_2	1	29.06	29.06	55.98	<0.0001
X^2_3	1	59.28	59.28	114.19	<0.0001

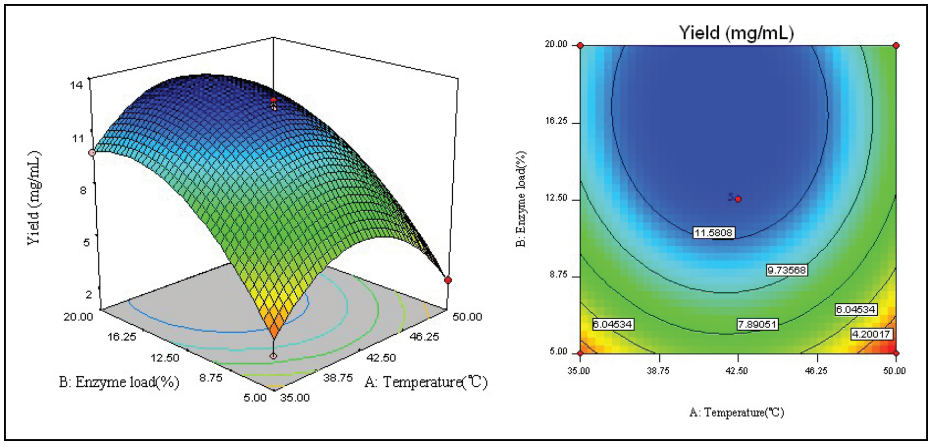

Fig. 1: Response surface plot and contour plot of reaction temperature and enzyme load.

Figure 3 indicates the interaction of enzyme load (X_2) and reaction time (X_3) on the yield of G-M1. The highest conversion yield could be achieved when using about 17 % of enzyme load and 19 h of reaction time. However, the conversion yield did not increase with the enzyme load over 17 %. Moreover, 19 h of reaction time is enough for enzymatic preparation to convert all Rd to G-M1.

2.4. Optimal conditions and model verification

The optimal conditions obtained from the model were as follows: reaction temperature of 41 °C, enzyme load of 17.5 % and reaction time of 18.3 h, respectively. The software predicted the yield of G-M1 was 14.07 mg/mL. In order to compare the predicted result with the practical value, as shown in Table 4, three parallel experiments were carried out using the optimal conditions. In average value of 13.89 mg/mL was observed from real experiments, which is in close agreement with the value predicted by the model equation. This indicated that the optimization is reliable in the present study.

2.5. HPLC analysis of the bioconversion process

HPLC analysis of the bioconversion of G-Rd to G-M1 was in accordance with our pervious report (Li et al. 2012). In brief, analysis was performed with a HPLC instrument (Agilent 1100, USA) equipped with a quaternary solvent delivery system, a column oven and UV detector. A HPLC method was developed using a reversed-phase C18 column (Hypersil ODS2, 250 mm × 4.6 mm I.D., 5 μm). The column temperature was set at

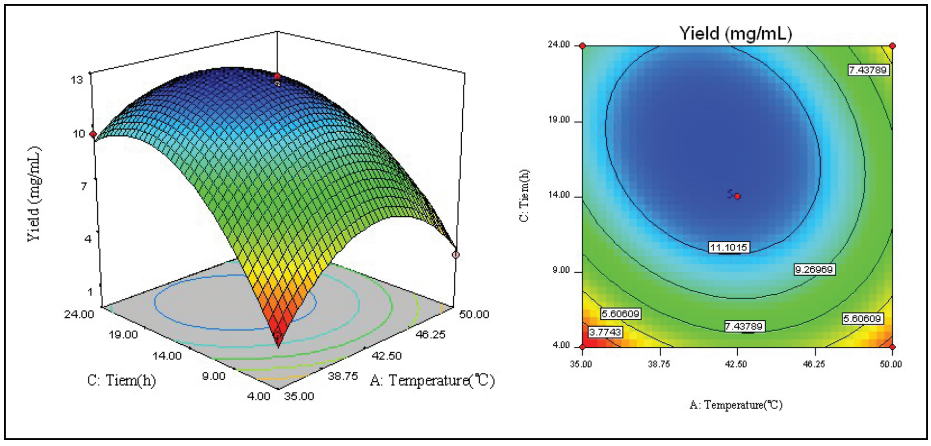

Fig. 2: Response surface plot and contour plot of reaction temperature and reaction time.

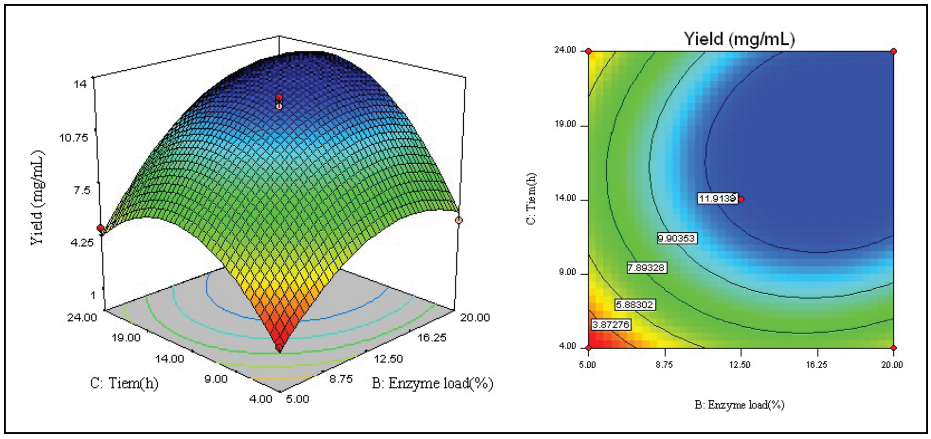

Fig. 3: Response surface plot and contour plot of enzyme load and reaction time.

Table 4: Optimum conditions and the predicted and experimental value of response at the optimum conditions

	Reaction temperature (°C)	Enzyme load (%)	Reaction time (h)	Yield of G-M1 (mg/mL)
Optimum conditions	41.02	17.51	18.27	14.07 (predicted)
Modified conditions	41.0	17.5	18.0	13.89 (actual)

room temperature and detection wavelength was set at 203 nm. The mobile phase consisted of 25 % acetonitrile and 75 % water with a flow rate of 1.0 mL/min. The 20 µL of sample solution was directly injected into the chromatographic column manually. A HPLC chromatogram is shown in Fig. 4.

2.6. Isolation and purification of G-M1

After termination of the enzymatic reaction, the reaction mixtures were evaporated in vacuo, suspended in water, and then partitioned between ethyl acetate and *n*-butanol. The *n*-butanol layer was loaded onto a silica gel column (80 cm × 3 cm, I.D.; solvent, $CHCl_3$: MeOH = 10:1) to give crude G-M1. The crude G-M1 was then separated and purified by semi- preparative liquid chromatography (mobile phase of 30% acetonitrile) to give G-M1 with purity more than 98.0%.

2.7. Cytotoxicity of G-M1 on MIN6 pancreatic β-cell

The G-M1 obtained as described in section 2.6 was used for cell experiments. To avoid excessive cytotoxicity at high doses,

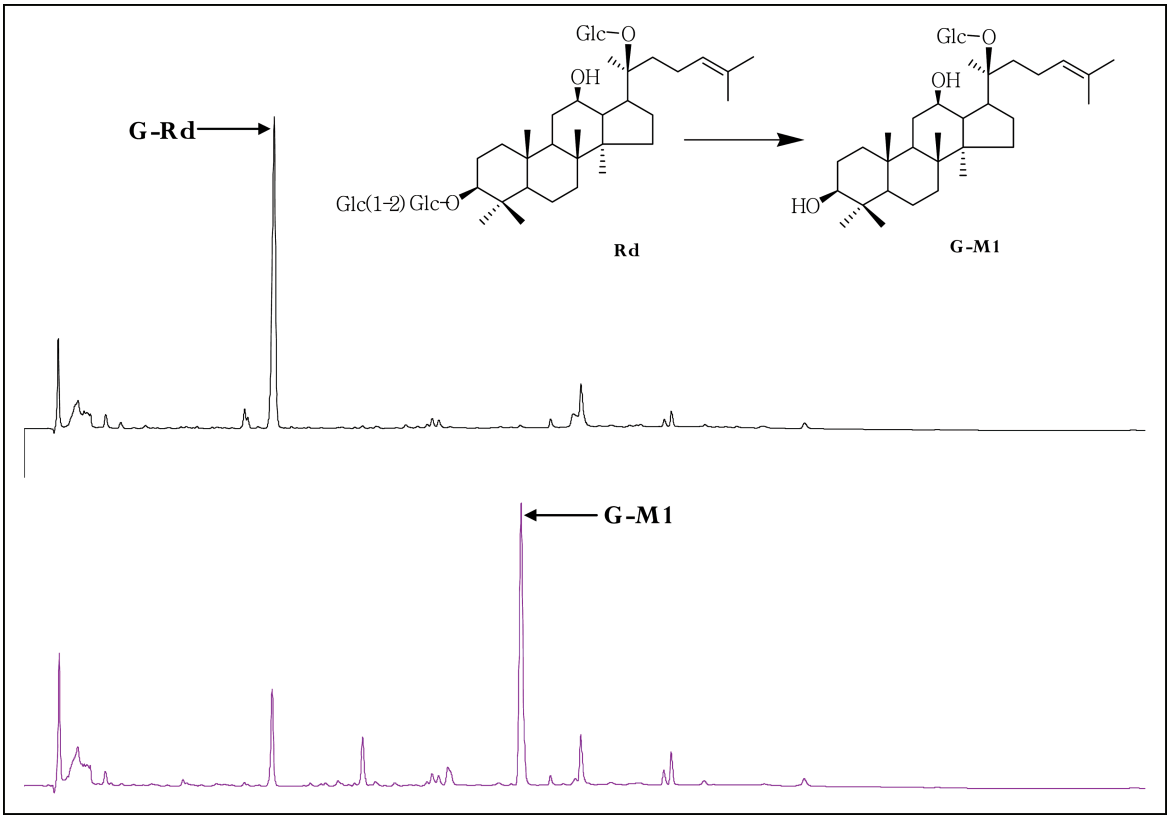

Fig. 4: HPLC analysis of the bioconversion of G-Rd to G-M1.

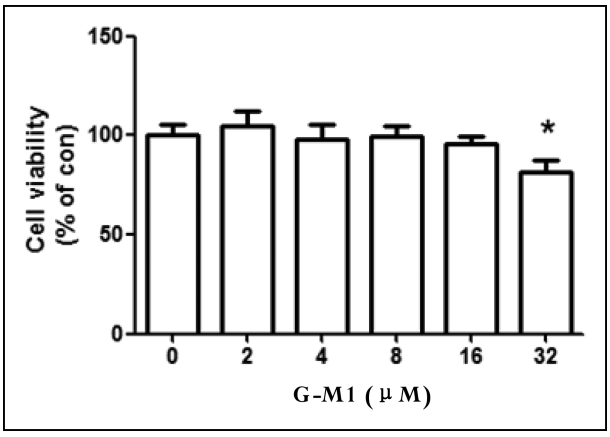

Fig. 5: Effect of G-M1 on cell viability of MIN6 Cells. MIN6 cells were treated with G-M1 for 24 h. Data was expressed as means ± SEM (n = 3), * $p < 0.05$, Compared with G-M1-0 μM group.

we firstly evaluated the possible cytotoxicity of G-M1 on MIN6 cells at various concentrations (2, 4, 8, 16, and 32 μM) for 24 h. The cell viability, expressed as percentage of the untreated control (100% cell viability), was investigated by MTT assay. As shown in Fig. 5, at the concentration 16 μM, G-M1 had little effect on the viability of MIN6 cells. However, when the concentrations reached 32 μM, G-M1 decreased the cell viability to around 83 %. Hence, we chose 8 μM of G-M1 for the following experiment.

2.8. Effect G-M1 on insulin secretion in MIN6 pancreatic β-cells

After incubation with G-M1 for 24 h, MIN6 cells were exposed to the low (3 mM) and stimulatory (30 mM) glucose concentrations. As shown in Fig. 6, G-M1-8 μM enhanced insulin secretion under both conditions, and the stimulation of insulin secretion of G-M1 under stimulatory glucose concentrations was significantly higher than that of control ($p < 0.05$). The result shows that G-M1 enhances glucose-stimulated insulin secretion in MIN6 pancreatic β-cells.

3. Discussion

Ginsenosides, the saponins from the roots of *Panax ginseng*, are the principal components responsible for the pharmacological and biological activities of ginseng. The pharmacological activities of ginsenoside are based on its metabolites formed by intestinal bacterial deglycosylation after oral administration (Hasegawa et al. 2004). Ginsenoside M1, referred to as compound K or IH901, was deemed as the major intestinal bacterial metabolite absorbed into the blood (Kang et al. 2013; Kim et al. 2014). So far, many investigations have shown that it is necessary for more effective *in vivo* physiological activities to convert ginsenosides into deglycosylated ginsenosides (Bae et al. 2002; Wang et al. 2011). Among many described methods, enzymatic bioconversion has been implicated as the most promising for minor ginsenosides *via* the selective hydrolysis of the sugar moieties of ginsenosides (Noh et al. 2009; Quan et al. 2011). The results showed that snailase can easily hydrolyze the sugar moiety of ginsenoside Rd with higher conversion rate.

Response surface methodology (RSM), an effective statistical technique, has been found to be a useful aid for studying the effect of several factors that influence the response of a system as well as optimizing the variables of a wastewater treatment process (Jentzer et al. 2015). Furthermore, it is essential to choose an appropriate experimental design method that will evaluate the effects of the major parameters involved in the treatment method and their probable interactions, through the minimum number of experiments. Box-Behnken design (BBD) as one of RSM is more efficient and easier to arrange and interpret experiments in comparison with others and widely applied to many studies (Lahlali et al. 2008). Our research team has employed this technology for the extraction processes (Li et al. 2011; Zhao et al. 2012). Here, the conditions for enzymatic preparation of G-M1 from G-Rd were optimized by using RSM and BBD. The results demonstrated that the change at reaction temperature, enzyme load and reaction time could significantly affect the yield of G-M1.

In our previous study, we have confirmed that G-M1 treatment increased the plasma insulin levels in the HFD/STZ mouse model (Li et al. 2012). Moreover, others have reported G-M1's insulin secretagogue effect on HIT-T15 cells (Han et al. 2007). Therefore, we further investigated the long-term effect of G-M1 on the insulin secretion by glucose-stimulated insulin secretion. In comparison with the Han's results, ginsenoside G-M1 with long-term action may also benefit the improvement on type 2 diabetes. In other words, G-M1 may ameliorate the function of pancreatic β-cells during the exposure to high glucose.

In a word, in the present study, ginsenoside Rd was converted into ginsenoside M1 by snailase hydrolysis for the first time. The conditions for enzymatic preparation of ginsenoside M1 were optimized by using response surface methodology. The estimated models were able to indicate preparation conditions, allowing superior conversion yield. The highest yields predicted for G-M1 could be attained under optimal conditions including 41 °C of reaction temperature, 17.5 % of enzyme load and 18 h of reaction time. Moreover, the present work indicates that G-M1 exerts prominent stimulatory effects on insulin secretion in MIN6 pancreatic β-cells.

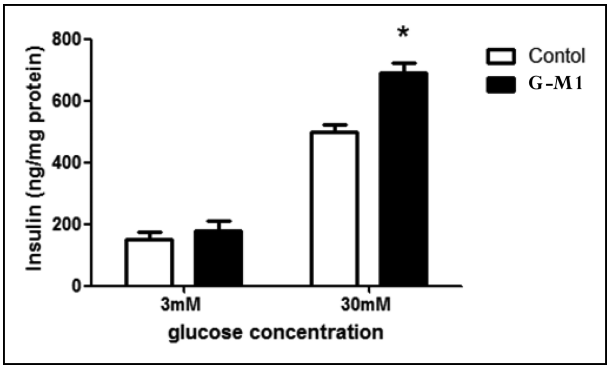

Fig. 6: . Effect of G-M1 on insulin secretion in MIN6 pancreatic β-cells. MIN6 cells were treated with G-M1 for 24 h. Data was expressed as means ± SEM (n = 3), * $p < 0.05$, Compared with Control group.

4. Experimental

4.1. Materials and chemicals

G-Rd was isolated and purified with the method described previously (Hou et al. 2010) and its structure was elucidated on the basis of spectroscopic method including UV, IR, MS, and ^{13}C-NMR. Standards of Rd and G-M1 were obtained from our lab. Snailase was purchased from Beijing Biodee Biotechnology Co., Ltd (http://www.biodee.net). β-Glucanase, cellulase and amylase were supported by Ningxia Xiasheng Group Co., Ltd.

HPLC-grade acetonitrile and methanol were purchased from Fisher Chemicals (USA). Other chemicals were all of analytical grade from Beijing Chemical Factory.

4.2. Enzymatic preparation of G-M1 from G-Rd

Snailase was incubated with G-Rd in a pH 4.5 sodium acetate buffer with agitation at different temperature (varying reaction temperature from 35 to 50 °C) and different enzyme load (varying from 5 to 20 %) for a certain time

(varying reaction time from 4 to 24 h). The mixture was subsequently placed in a water bath at 90 °C to terminate the enzymatic reaction. The reaction mixtures were individually evaporated, dissolved in methanol, and filtered through a 0.45 μm nylon filter membrane prior to injection into the HPLC system. The chromatographic peaks of G-Rd and G-M1 were confirmed by comparing their retention times with those of the reference standards. Quantification was carried out by the integration of the peak using external standard method.

4.3. Experimental design

In the present investigation, we employed the software Design Expert (Trial Version 7.1.6, Stat-Ease Inc., Minneapolis, MN) for experimental design, data analysis and model building. A Box-Behnken design (BBD) with three variables was used to determine the response pattern and then to establish a model.

Experimental data were fitted to a quadratic polynomial model and regression coefficient obtained. The non-linear computer-generated quadratic model used in the response surface was as follows:

$$Y = \beta_0 + \sum_{j=1}^{k} \beta_j X_j + \sum_{j=1}^{k} \beta_{jj} X_j^2 + \sum \sum_{i<j} \beta_{ij} X_i Y_j$$

where Y is the estimated response, β_0, β_j, β_{jj} and β_{ij} are the regression coefficients for intercept, linearity, square and interaction, respectively, while X_i, X_j are the independent coded variables.

4.4. Cell culture

MIN6 cell line was purchased from Xiangya Medical College of Central South University. The cells were grown in Dulbecco's modified Eagle's medium (DMEM 25 mmol/L glucose, GIBCO) equilibrated with 5 % CO2 and 95 % air at 37 °C. The medium was supplemented with 10 % fetal calf serum, 100 U/ml penicillin sulfate and 50 μg/mL gentamycin. All experiments were performed when the cells reached 80% confluence.

4.5. Insulin secretion assays

For insulin secretion experiments, MIN6 cells were seeded in 6-well plates. After 24 h incubation with G-M1-8 μM (the safe dose according to a preliminary experiment), the cells were pre-incubated at 37 °C for 0.5 h in Krebs-Ringer bicarbonate Hepes buffer (KRB; 129 mM NaCl, 4.8 mM KCl, 2.5 mM $CaCl_2$, 1.2 mM $MgSO_4$, 1.2 mM KH_2PO_4, 5 mM $NaHCO_3$, 10 mM Hepes, and 0.2% BSA). Cells were then treated in Krebs-Ringer bicarbonate Hepes buffer containing 3 mM or 30 mM glucose for 1 h. Cell supernatants were collected and centrifuged at 1000 rpm, 4 °C for 5 min. Insulin was measured by radioimmunoassay (RIA) (Tianjin Nine Tripods Medical & Bioengineering Co., Ltd, Tianjin, China).

4.6. Data analysis

Data were expressed as standard errors of the means (SEM) of three replicated determinations. The response obtained from each set of experimental design (Table 1) was subjected to multiple non-linear regressions using the Design Expert software. The quality of the fit of the polynomial model equation was expressed by the coefficient were checked by F-test and P-value. The significance level for all comparisons was $P < 0.05$.

Acknowledgments: This work was supported by General Financial Grant from the China Post-Doctorate Science Foundation (NO. 2012M520483) and the Open Project Program of State Key Laboratory of Food Science and Technology, Nanchang University (No. SKLF-KF-201211). National Key Technology Research and Development Program of the Ministry of Science and Technology of China (NO. 2011BAI03B0106).

References

Akao T, Kida H, Kanaoka M, Hattori M, Kobashi K (1998) Intestinal bacterial hydrolysis is required for the appearance of compound K in rat plasma after oral administration of ginsenoside Rb1 from *Panax ginseng*. J Pharm Pharmacol 50: 1155–1160.

Bae EA, Han MJ, Choo MK, Park SY, Kim DH (2002) Metabolism of 20 (S)- and 20 (R)-ginsenoside Rg3 by human intestinal bacteria and its relation to *in vitro* biological activities. Biol Pharm Bull 25: 58–63.

Han BH, Park MH, Han YN, Woo LK, Sankawa U, Yahara S, Tanaka O (1982) Degradation of ginseng saponins under mild acidic conditions. Planta Med 4: 146–149.

Han GC, Ko SK, Sung JH, Chung SH (2007) Compound K enhances insulin secretion with beneficial metabolic effects in *db/db* mice. J Agric Food Chem 55: 10641–10648.

Hasegawa H (2004) Proof of the mysterious efficacy of ginseng: basic and clinical trials: metabolic activation of ginsenoside: deglycosylation by intestinal bacteria and esterification with fatty acid. J Pharmacol Sci 95: 153–157.

Hou JG, He SY, Ling MS, Li W, Dong R, Pan YQ, Zheng YN (2010) A method of extracting ginsenosides from *Panax ginseng* by pulsed electric field. J Sep Sci 33: 2707–2713.

Liu X, Cui Y, Yang L, Yang SL (2005) Purification of a ginsenoside-Rb1 hydrolase from Helix snailase. Chin J Biotechnol 21: 929–933.

Jentzer JB, Alignan M, Vaca-Garcia C, Rigal L, Vilarem G (2015) Response surface methodology to optimise Accelerated Solvent Extraction of steviol glycosides from Stevia rebaudiana Bertoni leaves. Food Chem 166: 561–567.

Joh EH, Lee IA, Jung IH, Kim DH (2011) Ginsenoside Rb1 and its metabolite compound K inhibit IRAK-1 activation-The key step of inflammation. Biochem Pharmacol 82: 278–286.

Kang KA, Piao MJ, Kim KC, Zheng J, Yao CW, Cha JW, Kim HS, Kim DH, Bae SC, Hyun JW (2013) Compound K, a metabolite of ginseng saponin, inhibits colorectal cancer cell growth and induces apoptosis through inhibition of histone deacetylase activity. Int J Oncol 43: 1907–1914.

Kim DY, Park MW, Yuan HD, Lee HJ, Kim SH, Chung SH (2009) Compound K induces apoptosis *via* CAMK-IV/AMPK pathways in HT-29 colon cancer cells. J Agric Food Chem 57: 10573–10578.

Kim DY, Yuan HD, Chung IK, Chung SH (2009) Compound K, intestinal metabolite of ginsenoside, attenuates hepatic lipid accumulation *via* AMPK activation in human hepatoma cells. J Agric Food Chem 57: 1532–1537.

Kim JR, Choi J, Kim J, Kim H, Kang H, Kim EH, Chang JH, Kim YE, Choi YJ, Lee KW, Lee HJ (2014) 20-O-β-D-Glucopyranosyl-20(S)-protopanaxadiol-fortified ginseng extract attenuates the development of atopic dermatitis-like symptoms in NC/Nga mice. J Ethnopharmacol 151: 365–371.

Ko SR, Choi KJ, Suzuki K, Suzuki Y (2003) Enzymatic preparation of ginsenosides Rg2, Rh1, and F1. Chem Pharm Bull 51: 404–208.

Lahlali R, Massart S, Serrhini MN, Jijakli MH (2008) A Box-Behnken design for predicting the combined effects of relative humidity and temperature on antagonistic yeast population density at the surface of apples. Int J Food Microbiol 122: 100–108.

Lee IK, Kang KA, Lim CM, Kim KC, Kim HS, Kim DH, Kim BJ, Chang WY, Choi JH, Hyun JW (2010) Compound K, a metabolite of ginseng saponin, induces mitochondria-dependent and caspase-dependent apoptosis *via* the generation of reactive oxygen species in human colon cancer cells. Int J Mol Sci 11: 4916–4931.

Liu L, Wang Y, Peng C, Wang J (2013) Optimization of the preparation of fish protein anti-obesity hydrolysates using response surface methodology. Int J Mol Sci 14: 3124–3139.

Liu L, Zhu XM, Wang QJ, Zhang DL, Fang ZM, Wang CY, Wang Z, Sun BS, Wu H, Sung CK (2010) Enzymatic preparation of 20(*S, R*)-protopanaxadiol by transformation of 20(*S, R*)-Rg3 from black ginseng. Phytochemistry 71: 1514–1520.

Li W, Wang Z, Sun YS, Chen L, Han LK, Zheng YN (2011) Application of response surface methodology to optimise ultrasonic-assisted extraction of four chromones in *Radix Saposhnikoviae*. Phytochem Anal 22: 313–321.

Li W, Zhang M, Gu J, Meng ZJ, Zhao LC, Zheng YN, Chen L, Yang GL (2012) Hypoglycemic effect of protopanaxadiol-type ginsenosides and compound K on Type 2 diabetes mice induced by high-fat diet combining with streptozotocin *via* suppression of hepatic gluconeogenesis. Fitoterapia 83: 192–198.

Li W, Zhang M, Zheng YN, Li J, Wang YP, Wang YJ, Gu J, Jin Y, Wang H, Chen L (2011) Snailase preparation of ginsenoside M1 from protopanaxadiol-type ginsenoside and their protective effects against CCl4-induced chronic hepatotoxicity in mice. Molecules 16: 10093–10103.

Li W, Zhao LC, Wang Z, Zheng YN, Liang J, Wang H (2012) Response Surface Methodology to Optimize Enzymatic Preparation of Deapio-Platycodin D and Platycodin D from Radix Platycodi. Int. J. Mol. Sci 13: 4089–4100.

Noh KH, Oh DK (2009) Production of the rare ginsenosides compound K, compound Y, and compound Mc by a thermostable beta-glycosidase from Sulfolobus acidocaldarius. Biol Pharm Bull 32: 1830–1835.

Qi LW, Wang CZ, Yuan CS (2011) Isolation and analysis of ginseng: advances and challenges. Nat Prod Rep 28: 467–495.

Quan LH, Piao JY, Min JW, Kim HB, Kim SR, Yang DU, Yang D (2011) Biotransformation of ginsenoside Rb1 to prosapogenins, gypenoside XVII, ginsenoside Rd, ginsenoside F2, and compound K by *Leuconostoc mesenteroides* DC102. J Ginseng Res 35: 344–351.

Wakabayashi C, Hasegawa H, Murata J, Saiki I (1997) *In vivo* antimetastatic action of ginseng protopanaxadiol saponins is based on their intestinal bacterial metabolites after oral administration. Oncol Res 9: 411–417.

Wang L, Liu QM, Sung BH, An DS, Lee HG, Kim AG, Kim SC, Lee ST, Lm WT (2011) Bioconversion of ginsenosides Rb_1, Rb_2, Rc and Rd by novel β-glucosidase hydrolyzing outer 3-O glycoside from *Sphingomonas* sp. 2F2. Cloning, expression, and enzyme characterization. J Biotechnol 156: 125–133.

Wan JB, Zhang QW, Ye WC, Wang YT (2008) Quantification and separation of protopanaxatriol and protopanaxadiol type saponins from *Panax notoginseng* with macroporous resins. Sep Purif Technol 60: 198–205.

Yoon SH, Han EJ, Sung JH, Chung SH (2007) Anti-diabetic effects of compound K versus metformin versus compound K-metformin combination therapy in diabetic *db/db* mice. Biol Pharm Bull 30: 2196–2200.

You JY, Peng C, Liu X, Ji XJ, Lu J, Tong Q, Wei P, Cong L, Li Z, Huang H (2011) Enzymatic hydrolysis and extraction of arachidonic acid rich lipids from *Mortierella alpina*. Bioresour Technol 102: 6088–6094.

Zhao LC, He Y, Deng X, Xia XH, Liang J, Yang GL, Li W, Wang H (2012) Ultrasound-assisted extraction of syringin from the bark of *Ilex rotunda* Thumb using response surface methodology. Int J Mol Sci 13: 607–7616.

Zhao LC, He Y, Deng X, Yang GL, Li W, Liang J, Tang QL (2012) Response surface modeling and optimization of accelerated solvent extraction of four lignans from *Fructus schisandrae*. Molecules 17: 3618–3629.